Physics Letters A 374 (2010) 2248–2253

Contents lists available at ScienceDirect

Physics Letters A

www.elsevier.com/locate/pla

Sharp corners as sources of spiral pairs

Y. Biton [a], A. Rabinovitch [a,*], D. Braunstein [b], M. Friedman [c], I. Aviram [a,1]

[a] Physics Department, Ben-Gurion University of the Negev, Beer-Sheva 84105, Israel
[b] Physics Dept. Sami Shamoon College of Engineering, Beer-Sheva, Israel
[c] Department of Information Systems Engineering, Ben-Gurion University, Beer-Sheva 84105, Israel

ARTICLE INFO

Article history:
Received 13 January 2010
Received in revised form 21 March 2010
Accepted 22 March 2010
Available online 25 March 2010
Communicated by C.R. Doering

ABSTRACT

It is demonstrated that using the FitzHugh–Nagumo model, stimulation of excitable media inside a region possessing sharp corners, can lead to the appearance of sources of spiral-pairs of sustained activity. The two conditions for such source creation are: The corners should be less than 120° and the range of stimulating amplitudes should be small, occurring just above the threshold value and decreasing with the corner angle. The basic mechanisms driving the phenomenon are discussed. These include: A. If the corner angle is below 120°, the wave generated inside cannot emerge at the corner tip, resulting in the creation of two free edges which start spiraling towards each other. B. Spiraling must be strong enough; otherwise annihilation of the rotating arms would occur too soon to create a viable source. C. The intricacies of the different radii involved are elucidated. Possible applications in heart stimulation and in chemical reactions are considered.

1. Introduction

Excitable media are important in many areas. They appear in the heart [1], and in the nervous [2] and gastrointestinal [3] systems of the body, in Belousov Zhabotinsky and related chemical reactions [4], among others. The usual function of an excitable medium (EM) is related to the passage of excitation waves through it. When not stimulated, the EM stays quiescent. Below-threshold stimulation causes the appearance of a relatively small pulse, which promptly vanishes. Above-threshold stimulation produces a single wave, or a single burst of pulses which propagate through the EM, followed by a return to the resting state. This functioning is exhibited e.g. in the normal performance of the heart tissue and of the neurons in the body.

In certain unusual circumstances (see e.g. [5–7] for such conditions in the heart structure), a *permanent* source of waves can form in an EM. Such a source repeatedly emits waves which regularly propagate through the medium. If this phenomenon occurs, it may cause e.g. undesirable malfunctions in the heart (tachycardia and even fibrillation). A permanent source can be induced either by a regular (extrinsic or intrinsic) pace-maker, by boundary conditions, or by the creation of a *self-sustained* spiral or spiral-pair source.

Spiral pairs can be generated by several different methods [8]. Here we shall describe a new procedure to induce spiral pair source creation, based on what we would like to call the "corner effect".

2. The corner effect

Consider a triangular region, subsequently referred to as the "corner", shown in Fig. 1, embedded in a 2D excitable medium. During a very short period of time, an external stimulation impulse is applied in the corner throughout the triangular area depicted in Fig. 1. The stimulation amplitude, just above the activation threshold, is chosen in a small range, to be defined exactly in the following. Outside the corner region the medium is quiescent, while the excitability is the same both inside, and outside the corner, at all times. In order to be specific we use the FitzHugh–Nagumo system [9] to characterize the medium:

$$\frac{\partial v}{\partial t} = D\left(\frac{\partial^2}{\partial x^2} + \frac{\partial^2}{\partial y^2}\right)v + v(v-a)(1-v) - w + \delta(t)I(x,y),$$
$$\frac{\partial w}{\partial t} = \varepsilon(v - dw), \tag{1}$$

where all variables are dimensionless. Here, v is the action potential, while w is the refractivity, an inhibitory variable, $\delta(t)I(x,y)$ is the input current, or impulse. The constants D, a, and ε are the diffusion constant, the excitability parameter, and the ratio between the fast and the slow time constants respectively. The constant

* Corresponding author. Tel.: +97286461172; fax: +97286472903.
E-mail address: avinoam@bgu.ac.il (A. Rabinovitch).
[1] Guest.

0375-9601/$ – see front matter
doi:10.1016/j.physleta.2010.03.045

d controls the shape of the wave. Here $\delta(t)$ is the Dirac delta function and $I(x, y)$ is a constant of magnitude A, inside the corner, and zero elsewhere. The corner is part of an excitable square domain, obeying Neumann boundary conditions on all sides. All following calculations were carried out with the parameter values $a = 0.12$, $D = 0.2$, $\varepsilon = 0.005$, $d = 3$. The system of equations was solved by using a second order Euler finite difference scheme with time and spatial increments $\Delta t = 0.125$, $\Delta x = \Delta y = 0.5$ over a grid of 400×400 points. It was verified that moving the corner vertex along the x axis direction from $(0, 0)$ did not change results. Table 1 summaries the definitions of parameters and abbreviations used in this study.

Table 1
List of definitions and abbreviations.

Variable	Definition
A	Stimulation amplitude
A_c	The lowest (critical) stimulation amplitude for the corner effect
A_c^+	Stimulation amplitude just above A_c
A_f	The upper value of A for the corner effect
ALP	Arc-like pulse, a structure (see Ref. [10]) capable of creating a spiral-pair source
α	Corner's angle
C, V_n	Velocity of a *plane* wave and normal velocity of a wave in an excitable medium, respectively
R^*	The smallest radius of a wave (measured where $v > 0.1$) after stimulation and before its outwards propagation
$R_0 = R_{cr}^+$	A radius just above R_{cr}
R'	Radius of a circular path followed by the tip of each spiral arm
$R_{cr}(A)$	Same as R'_{cr} but as a function of the stimulating amplitude
R'_{cr}	Minimum (critical) radius of a stimulated circular area for producing a propagating wave
R_{eff}	Radius of a circle having the same area as that of the maximum area in the corner where no wave appears (Fig. 7)
R_f	See inset (Fig. 6)
R_r	Radius of the smallest circle within a corner where a wave can emerge (Fig. 1a) and also the radius of a "corner rounding circle" (Fig. 10)
ℓ	Distance from corner vertex along which no wave can emerge (see inset, Fig. 6)
K	Wave curvature
v	Action potential (in the heart or neurons)
VF	Ventricular fibrillation
FHN	FitzHugh–Nagumo

We wish to explore the effect of a corner in generating a *permanent source of waves*. Such a source appears only for stimulations *just above* the activation threshold A_c, typical of the medium. Thus, following a single stimulation impulse with $A < A_c$, the activity, consisting of v and w of Eq. (1), ultimately collapses to zero; a single stimulation with $A \gg A_c$, on the other hand, produces a single outgoing pulse, which disappears at the boundary of the medium; only when the stimulation A is slightly larger than A_c, the corner shaped stimulation is able to generate a stable source.

Figs. 1–3 show the three cases, $A < A_c$ (Fig. 1), $A_c < A < A_f$ (Fig. 3), where A_f is the highest value of A for which a spiral pair source ensues, and $A > A_f$ (Fig. 2). For all values of A, the dynamics is as follows: the maximum of v in the corner is at first drawn inwards, due to the out-going diffusion current. The maximum of v increases thereafter inside the corner, simultaneously building up the refractivity w. The latter causes v to decrease inside the corner. When $A < A_c$ (Fig. 1) both v and w eventually disappear. For $A > A_f$ (Fig. 2) a single, continuous wave propagates outwards, without any free edges, or splits (see below) being created. We now concentrate on the behavior for the values $A_c < A < A_f$ (Fig. 3).

The actual wave patterns developed in this region are quite complex. The combined action of the increase in w and the *corner shape effect* leads to the formation of two segments of small width and *finite* length (i.e. they possess free edges), which cannot re-enter the vertex of the corner (see below). These edges spiral towards each other, eventually generating the spiral-pair source. The precise shape and size of the corner region where the effect is valid will now be discussed.

Fig. 4 describes the threshold level A_c and the range of A values, up to A_f, where a permanent source of spiral-pairs is obtained for an excitability value of $a = 0.12$ in Eq. (1). The results

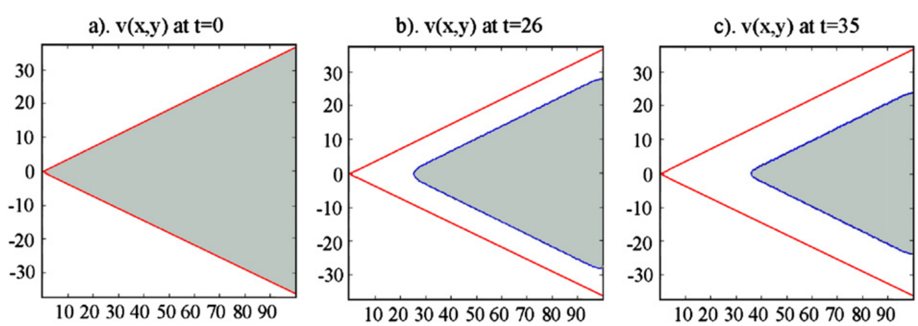

Fig. 1. Time evolution of $v(x, y)$ for the case of $A = 0.1550 < A_c = 0.1555$ and $\alpha = 40°$. The corner border is shown in red, while the shaded area outlined in blue represents $v(x, y) > 0.1$ at successive times. (For interpretation of the references to color in this figure legend, the reader is referred to the web version of this Letter.)

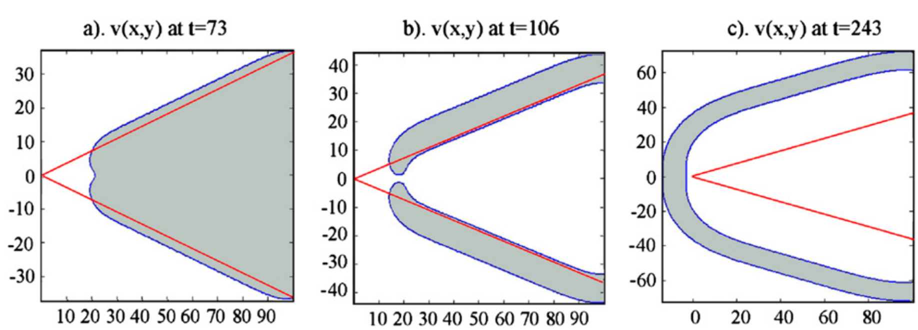

Fig. 2. Time evolution of $v(x, y)$ for the case of $A = 0.1575 > A_f = 0.1566$ and $\alpha = 40°$. The corner is depicted in red, while the shaded area outlined in blue represents $v(x, y) > 0.1$ at successive times. Note the change of scales in b,c, made in order to include the whole wave. (For interpretation of the references to color in this figure legend, the reader is referred to the web version of this Letter.)

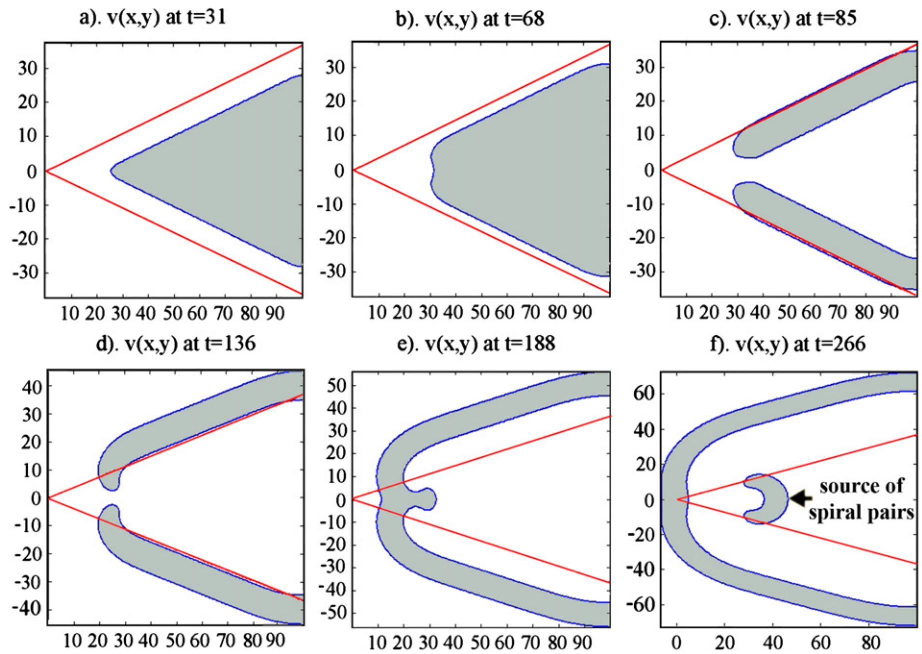

Fig. 3. Time evolution of $v(x, y)$ for the case of $A_c < A = 0.1560 < A_f$ and $\alpha = 40°$. The corner is depicted in red, while the shaded area outlined in blue represents $v(x, y) > 0.1$ at successive times. Note the changes of scales in d–f. (For interpretation of the references to color in this figure legend, the reader is referred to the web version of this Letter.)

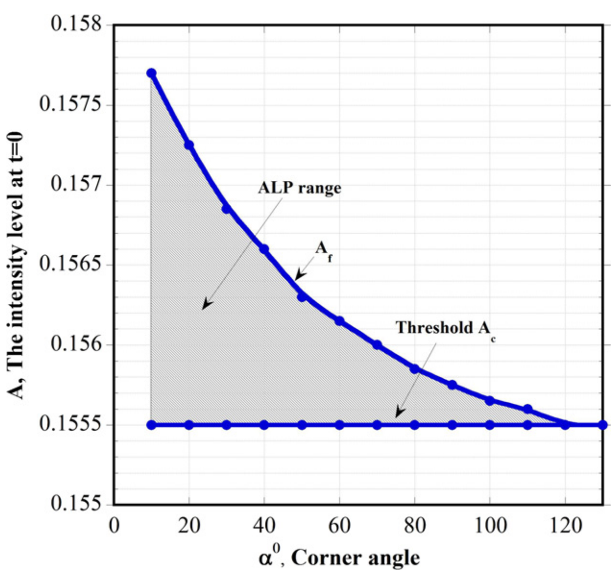

Fig. 4. The range of amplitudes A generating a spiral-pair source via sharp corners. Note that below $\alpha = 10°$ the structures become too narrow.

of numerical integration being sensitive to the grid density used for the purpose, the number of grid points inside the narrow region of the corner's vertex depends on the unit cell dimensions, which could distort the resolution. The results in Figs. 1–3 were obtained with the same unit cell for all corner angles, and it was verified that halving the cell size caused relative changes of less than 10^{-4}. It is clear that: (a) The threshold, A_c, is angle independent. (b) The range of stimulation amplitude in which a perpetual source can be generated is indeed very small, and its discovery therefore has probably been missed till now. (c) The range of the stimulation amplitude increases with decreasing angles from ~ 0 at 130°, to ~ 0.022 at 10°. Following is an explanation of the underlying mechanism of this corner effect.

We propose that the effect is largely the outcome of a combination of the following two well-known processes: (1) Due to their high curvature near the vertex of the corner, the waves generated by the stimulation cannot emerge there, and consequently segments with free edges are symmetrically created on both sides of the corner. (2) These free edges proceed to spiral towards each other since they are slower than the rest of the outgoing waves. The condition for this spiraling to induce a permanent source is that a viable arc-like pulse (ALP [10]) be created. We will show, however, that details are important to provide a better understanding of the sequence of events.

2.1. The curvature

It is well known [11] that, in order to obtain a viable propagating wave in an excitable medium, a stimulating current of a specific amplitude, A, should be applied to a minimal ("liminal") area [12], characterized by its critical radius R'_{cr},[2] which is the minimum radius of a circle of this area. A similar radius can be defined by measuring the minimum size, $\sim 2R'_{cr}$, of a gap (isthmus) through which a plane wave can pass [13]. A minimum radius is also inferred from the maximum curvature a wave can have. According to the Eikonal equation, the normal velocity V_n of a wave in an excitable medium [14] is given by:

$$V_n = C - Dk, \tag{2}$$

where C is the velocity of a plane wave, D is the diffusion coefficient and $k = 1/R$ is the wave curvature. A minimum R is obtained for $V_n = 0$, i.e. for $R'_{cr} = D/C$.

The dependence of R'_{cr} on the stimulation amplitude is of major importance here. However, both methods discussed above to obtain R'_{cr} treat a fully developed pulse or a large A. We intend to find the minimal radius, $R_{cr}(A)$ for threshold and near threshold values of A.

Consider a situation where a stimulation of amplitude A is applied in a disc of radius R within an excitable medium (Fig. 5a).

[2] Note that this and the next critical radii are designated by a prime to distinguish them (see below) from the critical radii relevant to this work.

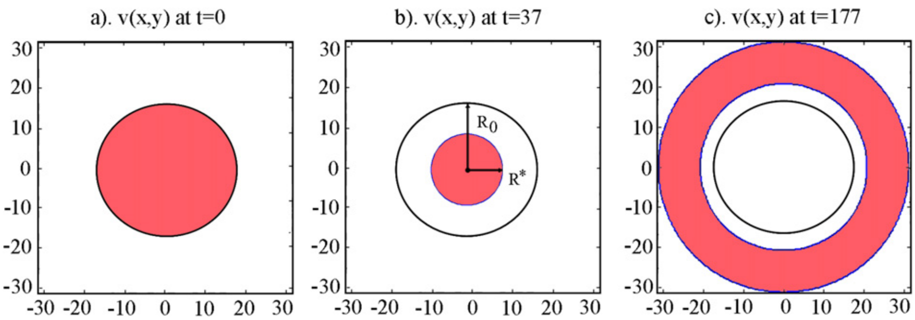

Fig. 5. Evolution of $v(x, y)$ from a stimulation of a disc of a radius just above threshold ($R_0 = R^+_{cr}$) for $A = 0.1560$. $v(x, y)$ is shown as a contour within which $v > 0.1$ (in red). a) The stimulation at $t = 0$. b) The minimum size situation. c) The outgoing ring (target wave). For this A value, $R_0 = 13$ and the minimum radius is $R^* = 6.4$. (For interpretation of the references to color in this figure legend, the reader is referred to the web version of this Letter.)

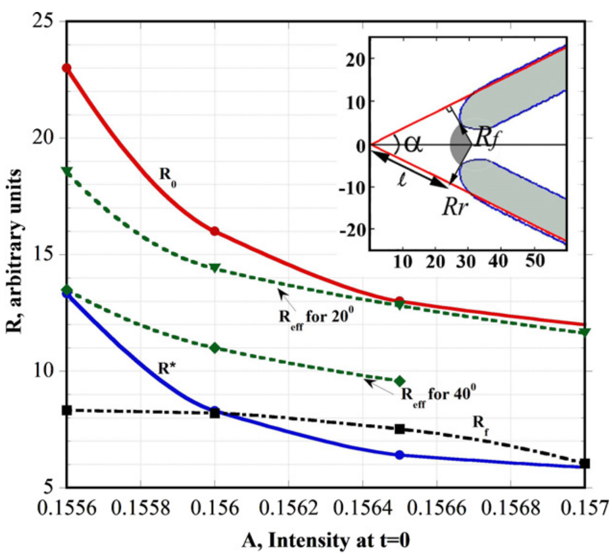

Fig. 6. The different critical radii as functions of A (see text).

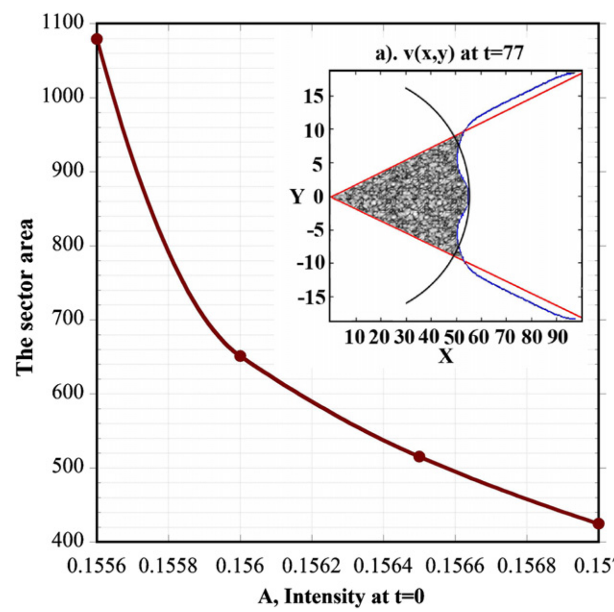

Fig. 7. The effective area of a 20° corner as a function of A. Inset a): Effective area ($S = 516$) for $A = 0.156$, $R_{eff} = 12.81$; $v(x, y)$ is drawn as a blue contour within which $v = 0.1$. (For interpretation of the references to color in this figure legend, the reader is referred to the web version of this Letter.)

The time evolution of $v(x, y)$ depends on R. For the case of $R < R_0$ (not shown), the activity decays to zero, and no outgoing pulse is created. However, for $R > R_0$ (see Figs. 5b and 5c in which we set $R = R_0$, just above R_{cr}) the initial behavior is similar to that found for a corner for which $A > A_c$, namely, the space of the action potential first decreases as a result of the outgoing diffusion current (Fig. 5b). The value of w in the interior then increases lowering v there, and leaving only a ring of v (see Fig. 5c). We designate the minimal radius of the action potential just before it develops into the mentioned ring by R^*, which is smaller than the initial radius R_0 (Fig. 5b). *With no corners disturbance* the ring progresses outwards as a (single) target wave.

For a specific A two critical radii can thus be defined: (1) $R_0(A)$ the disk radius for which this A is the threshold and (2) $R^*(A)$ the minimum radius to which the v-disc shrinks (Fig. 5a), just before turning to a ring. These critical radii are shown in Fig. 6 (together with additional radii to be discussed below). It is seen that R_0 values change approximately as $A^{-1/2}$, as can be expected if stimulation *area* is the determining factor. The amount of ingoing length $L = R_0 - R^*$ decreases slowly with A.

For a corner of angle α (Fig. 6, inset) we assume that near the corner's vertex there is a curvature of radius R_r, below which waves cannot form. In a region of length $\ell = R_r \cot(\alpha/2)$ from the vertex along the corner's sides the wave cannot emerge (see Section 2.3 for another definition of R_r). Consequently, following a usual contraction and the creation of a w-wave inside (see above), segmented waves of *finite lengths* emerge on both sides of the corner, each having a free edge. These waves move away from the corner causing the slower moving free edges to spiral in the opposite direction, i.e. inwards. The "forbidden" radius R_f for the corner is considered at the time where the two segments have already been created, and are just about to begin their spiraling (inset, Fig. 6). R_f is calculated by the distance from one contour tip to the intersection of the two normals from the tips to the corner sides. As expected, it is found (Fig. 6) that R_f depends imperceptibly on the corner's angle, and decreases with increasing stimulation amplitude. Its magnitude is also quite close to that of R^*.

A different approach to compare the corner effect with the radii R^* and R_0, could be based on comparing *areas*, as follows. Consider a corner situation, where $v(x, y)$ has shrunk to its minimal size, just before it develops into the two free edges (see Fig. 3b, and the inset of Fig. 7). We introduce a circular sector centered at the vertex of the corner having a radius equal to the largest distance between the vertex and the curve of $v(x, y)$ along the x direction (shaded region in the inset of Fig. 7). This area should be compared to the largest disc area below threshold. Fig. 7 displays this area as a function of A for a corner of 20°. We define an effective radius, R_{eff} of a circle having the same area as the circular sector. Fig. 6 shows R_{eff} as a function of A for corners of both 20°, and 40°. It is evident that the area approach is not appropriate here, since R_{eff} depends on the corner's angle.

2.2. Tip motion

After formation, the two segments start to propagate. For $A = A_c^+$, each tip moves in a small circle, as described in Ref. [15]. In order to clarify this motion, a corner of 40° was selected, and after the formation of the two disjoint segments on both sides of the corner, the top segment was completely discarded from the system, while the remaining segment was allowed to move on. Fig. 8 displays, for $\alpha = 40°$ and $A = 0.1555$, the movement of the lower segment (measured at $v = 0.1$) at successive times, from $t = 10$ to $t = 100$, separated by time intervals of $\Delta = 10$. It is seen that the tip moves around a small circle.

For higher A values, the radius of final rotation of the tip changes only slightly, since the change in A for the whole range of the ALP is very small (see [16] for the dependence of this radius on the system parameters). However, it is the *transient* movement of the tip before its final rotation which is the cause for the inability to create an ALP for higher A values, as can be seen in Fig. 9. The latter displays, by the method described in Ref. [17] the transient tip motion for increasing values of A. The initial position is marked by O, and successive numbers and arrows describe the trajectory direction. The tip location was calculated at successive time intervals of width $\Delta = 5$, from $t = 0$ up to $t = 600$. Note [10] that, it is the *arms* of the two spirals, which eventually collide and are mutually annihilated. To produce a viable ALP, however, the tip zone must have enough free room in order to avoid destruction in the process. These 'tip zones' of the segments move symmetrically, but their motion depends on the initial value of A. Thus, for $A = A_c^+$, each tip zone moves along a simple circle [15]. For higher A values they move on oval shaped trajectories which eventually settle down onto circular orbits centered at different locations than the one for $A = A_c^+$ (Fig. 9). It is this pair of oval trajectories which controls the creation of an ALP, since the two segments collide while still moving on them. Before collision the relative motion of the tips is such that the distance between them decreases. If collision occurs at this stage, i.e. the tips themselves have collided (option 1), no ALP can be created since the tips annihilate each other. If the conditions for option 1 do not apply, then the free tips continue their own spiraling trajectory, the relative motion of the tips reversing sign, and the distance between them increases. If a collision (and annihilation) occurs at this stage (option 2) it will have affected portions of spirals *behind* the tips. The tips break away from the original spirals, and a viable ALP can emerge. The final oval shaped stage of the trajectory before collision can be locally approximated by a circle of radius R' as suggested in Fig. 9. It was verified numerically that R' barely changes with A. The feature that does change is the *center* of this circle. With increasing A these centers approximately move along a straight line (the centers' locus) with a slope of $\sim\alpha/4$ in the direction of the corner vertex. The shortest distance between tips thus decreases with increasing A and therefore for $A > A_f$, option 1 is realized. Otherwise ($A_c < A < A_f$) option 2 takes place.

2.3. How sharp should a corner be?

Is a rounded corner as efficient in spiral pair creation as a sharp one? In order to answer this query we ran a set of 40° corners, with rounded vertices, and recorded the A_f as a function of the radius, R_r of the rounding (Fig. 10). It is seen that below $R_r = 7$, almost no change in A_f is detected, i.e. the corner is sharp enough. The difference between the A_f values for $R_r = 7$ to $R_r = 0$ is about $3.5 \cdot 10^{-5}$. This value of $R_r = 7$ is to be compared with R_f for $A = 0.15660$ (see Fig. 6). For larger R_r values there is a gradual decrease of A_f until $R_r > 22$ beyond which the ALP is no longer

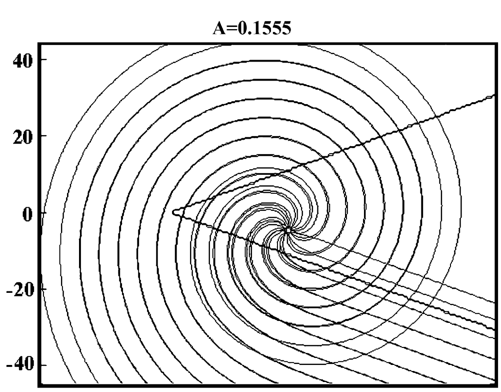

Fig. 8. Successive contours of $v = 0.1$ drawn from $t = 10$ to $t = 100$ separated by time intervals of $\Delta = 10$ for $\alpha = 40°$ and $A = 0.1555$. The assembly of tips describes a movement around a small circle.

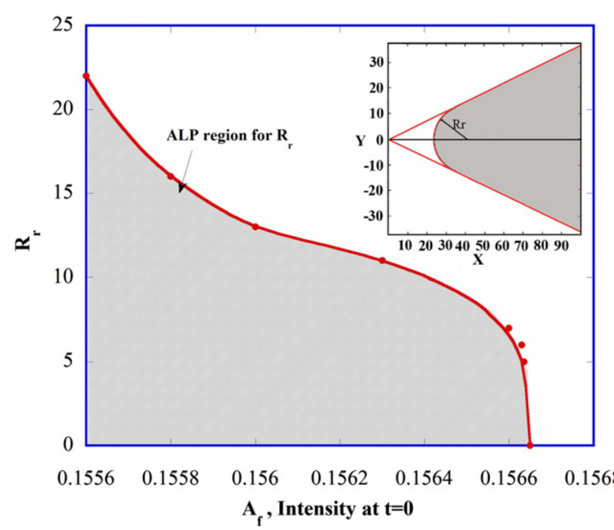

Fig. 10. The radius R_r (red points) of rounding of a corner of 40° as a function of A_f. The smooth curve serves only as a guide to the eye. (For interpretation of the references to color in this figure legend, the reader is referred to the web version of this Letter.)

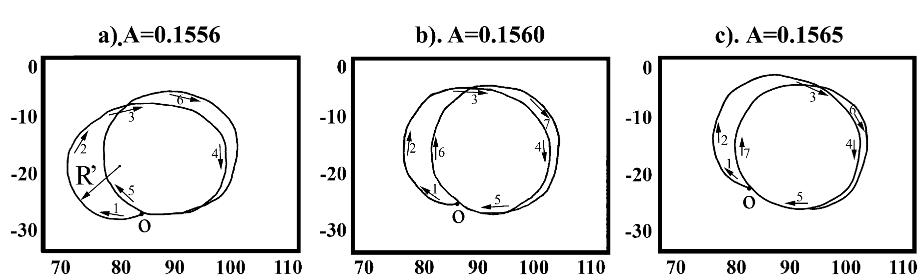

Fig. 9. Tip motion for $\alpha = 40°$ and different values of A. Only the movement of the *lower* segment is presented. The initial point of movement is marked by O. The trajectory traced out by the tip is shown by successive numbers and arrows.

created, i.e. $A_f = A_c$. This R_r value is to be compared to the value of R_0 for A_c (see Fig. 6).

In order to check self-consistency, consider e.g. the case where, ℓ, the distance from the corner vertex along its side, where waves cannot emerge, equals 19.3. From the insert in Fig. 6, this ℓ value corresponds to $R_r = 7$ for $\alpha = 40^\circ$ and to $R_r = 13.5$ for $\alpha = 70^\circ$. According to Fig. 4, the A_f values for these α are 0.1566 and 0.1560 respectively. Now, from Fig. 10, these A_f correspond to R_r of 7 and 13.5 as obtained above.

3. Applications

The method of spiral creation described here can be useful for several reasons: (a) it is quite easy to use this method to create double spirals in numerical simulations, in experimental arrangements it can be implemented by using electrodes of, say, triangular or square shapes: (b) it may be used in chemical reactions such as the Belousov–Zhabotinsky ones [18] to induce spiral pairs and (c) it may be useful in heart studies such as [19], instead of the current method of inducing VF by rapid pacing.

The use of this method experimentally should however be treated with caution. Firstly, the method was developed only for the FHN system and therefore may be inapplicable in other systems, although the FHN was shown (see e.g. [20]) to be broad enough to model many experimental arrangements. Secondly, e.g. in cardiac tissue, intrinsic heterogeneity in experimental preparations could cause spatial variations in the stimulus threshold larger than the A_f–A_c range. Moreover, the tissue response below the stimulating electrode is usually complex [21] and it may generate “secondary sources” [22]. The method applicability should also be checked in non-stationary (e.g. living) media and under anisotropic and asymmetric conditions.

4. Conclusions

Sharp corners have been shown to be possible birthplaces for double spiral sources at least for the FHN model. The procedure described here to obtain these spiral pairs seems to be *an easy way* to artificially create double spirals in an excitable medium. Although the range of stimulation amplitude values for such a creation is rather small (on the order of 1% of the threshold stimulus), the conditions for source creation are that they should be *just above* threshold values, a task which is not too difficult to achieve: It is quite easy to find the threshold amplitude, and then to apply a stimulation amplitude just a bit higher. Too high an amplitude is immediately detected by the appearance of *a single* target wave. The process of creation was analyzed in detail revealing several hidden mechanisms.

References

[1] See e.g. E.M. Cherry, F.H. Fenton, New J. Phys. 10 (2008) 125016;
B.F. Yang, Y.J. Lu, Z.G. Wang, Cardiovasc. Res. 79 (2008) 571, for more recent reviews.
[2] D.J. Shultz, J. Exp. Biol. 209 (2006) 4821;
J.C. Rekling, G.D. Funk, D.A. Bayliss, X.W. Dong, J.L. Feldman, Physiol. Rev. 80 (2000) 767.
[3] See e.g. W.J.E.P. Lammers, L.K. Cheng, Biomed. Eng. Online, Art #2 Jan, 2008;
R.J. Stevens, N.G. Publicover, T.K. Smith, Nature 399 (1999) 62.
[4] A.S. Mikhailov, K. Showalter, Phys. Rep. 425 (2006) 79;
A.F. Taylor, Prog. React. Kinet. Mech. 27 (2002) 247.
[5] E.M. Cherry, F.H. Fenton, Am. J. Physiol.-Heart Circ. Physiol. 292 (2007) H43.
[6] C. Antzelevitch, Heart Rhythm 2 (2005) S9.
[7] B. Swynghedauw, Physiol. Rev. 79 (1999) 215.
[8] E.M. Cherry, F.H. Fenton in Ref. [1];
A. Rabinovitch, M. Gutman, Y. Biton, I. Aviram, D.S. Rosenbaum, Phys. Rev. E 74 (2006) 061904;
Y. Biton, A. Rabinovitch, I. Aviram, D. Braunstein, Phys. Lett. A 373 (2009) 1762.
[9] See e.g. J.D. Murray, Mathematical Biology, 2nd ed., Springer-Verlag, Berlin, 1993, p. 161.
[10] A. Rabinovitch, Y. Biton, M. Gutman, I. Aviram, Comput. Biol. Med. 39 (2009) 405.
[11] C. Cabo, A.M. Pertsov, W.T. Baxter, J.M. Davidenko, R.A. Gray, Cir. Res. 75 (1994) 1014.
[12] W.A.H. Rushton, Proc. R. Soc. London B Biol. Sci. 124 (1937) 210;
H.A. Fozzard, M. Schoenberg, J. Physiol. (London) 226 (1972) 593.
[13] C. Cabo, A.M. Pertsov, W.T. Baxter, J.M. Davidenko, J. Jalife, Chaos 8 (1998) 116;
M. Wellner, O. Berenfeld, Theory of reentry, in: Cardiac Electrophysiology: From Cell to Bedside, 4th ed., Saunders, 2004, p. 317, especially notice Fig. 35-5 there.
[14] V.S. Zykov, Simulation of Wave Processes in Excitable Media, Manchester Univ. Press, Manchester, 1987.
[15] See e.g. V.G. Fast, A.G. Kleber, Card. Res. 33 (1997) 258, especially Fig. 7 therein.
[16] J.M. Starobin, C.F. Starmer, A.J. Starobin, Phys. Rev. E 56 (1997) R3757.
[17] R.A. Gray, A.M. Pertsov, J. Jalife, Nature 392 (1998) 75.
[18] See e.g. V.K. Vanag, I.R. Epstein, Chaos 18 (2008) 026107.
[19] See e.g. K. Nanthakumar, G.P. Walcott, S. Melnick, J.M. Rogers, M.W. Kay, R.E. Ideker, W. Holman, Heart Rhythm 1 (2004) 14.
[20] C. Vilas, M.R. Garcia, J.R. Banga, A.A. Alonso, Physica D 237 (2008) 2353.
[21] S.G. Patel, B.J. Roth, IEEE Trans. Biomed. Eng. 47 (2000) 1284.
[22] V.G. Fast, S. Rohr, A.M. Gillis, A.G. Kleber, Circ. Res. 82 (1998) 375.